Vego, I. *et al.* (2025) ***Géotechnique Letters*** **15**, 000–000, https://doi.org/10.1680/jgele.24.00063

A simple discrete approach to explore the response of swelling and softening particles

ILIJA VEGO*, VINCENT RICHEFEU†, GEORGIOS FELEKIS‡, ALESSANDRO TENGATTINI§ and GIOACCHINO VIGGIANI‖

The response of granular materials is significantly affected by the stiffness of the particles that constitute them. This stiffness can evolve and the particles can exhibit strong inter-granular strain. While generally overlooked in literature, these features emerge in numerous materials that can soften and swell. This is the case for clays, root systems, and polymer-based particles. This study investigates the macroscopic effects of concurrent particle swelling and softening, based on previous experimental results on hygroscopic granular assemblies. The material studied therein shows a dilation–compaction response in oedometric conditions, despite the constant load, driven by the evolving properties of the particles. To model this complex response, an intentionally simple discrete element approach is proposed, with variables depending on one main parameter. A sensitivity analysis – built on the proposed material model and implemented within the discrete element method approach – successfully reproduces the experimental observations and notably the dilation–compaction response. An analytical one-dimensional model is then developed to further explore the role of variables in such assemblies. The study highlights that a simple model can capture the experimentally observed meso-scale mechanisms, underlining how complex responses can emerge from elementary inter-particle interactions.

KEYWORDS: granular materials; modelling; moisture-related properties; softening; swelling

NOTATION

F	applied vertical force
h	height of an assembly of particles
h_0	height of an assembly of particles when $x = 0$
K	stiffness of the 1D system
K_0	stiffness of the 1D system when $x = 0$
k	particle stiffness, dependent on x
k_0	particle stiffness when $x = 0$
p	vertical stress
$\hat{p}$	critical or reference vertical stress
r	particle radius, dependent on x
t	time
u	particles overlap
x	main variable
r_0	particle radius when $x = 0$
u_0	particle overlap when $x = 0$
x_{MAX}	maximum asymptotic value of x
γ_K	coefficient modulating the 1D system stiffness decrease
γ_k	coefficient modulating the particle stiffness decrease
α_r	coefficient describing the relationship between x and r
β_K	ratio between $K(\infty)$ and K_0
β_k	ratio between $k(\infty)$ and k_0
Δh	height variation of an assembly of particles $(h - h_0)$
ε_n	height variation of the 1D system
μ	friction coefficient
ρ	particle density
τ	coefficient modulating the increase of x with time

Manuscript received 13 May 2024; accepted 11 October 2024.
First published online 13 December 2024.
*School of Civil Engineering, The University of Sydney, Sydney, Australia; Université Grenoble Alpes, Grenoble INP, CNRS, Grenoble, France (Orcid:0000-0003-4426-3382).
†Université Grenoble Alpes, Grenoble INP, CNRS, Grenoble, France (Orcid:0000-0002-8897-5499).
‡Université Grenoble Alpes, Grenoble INP, CNRS, Grenoble, France
§Université Grenoble Alpes, Grenoble INP, CNRS, Grenoble, France; Institut Laue-Langevin (ILL), Grenoble, France; Institut Universitaire de France (IUF), Paris, France (Orcid:0000-0003-0320-3340).
‖Université Grenoble Alpes, Grenoble INP, CNRS, Grenoble, France (Orcid:0000-0002-2609-6077).

INTRODUCTION

When modelling the mechanical behaviour of granular materials, it is typically assumed that the individual particles are rigid and their properties immutable. Inter-particle interactions generally receive much attention, as they play a crucial role in driving the macroscopic response of granular materials. This is particularly true for thoroughly studied granular materials such as sand and gravel. Nevertheless, a variety of other granular materials comprise 'active' constituents such as clay, roots, super-absorbent polymers, and biological or organic matter (Aguilera *et al.*, 1995; Romero *et al.*, 2011; Sweijen *et al.*, 2017; Saha *et al.*, 2020; Kolb *et al.*, 2022). The properties of the particles composing these materials vary with time, for example, in the presence of a triggering agent, such as water, which can alter their stiffness and their volume. This diverse group of materials is relevant for domains well beyond the geotechnical field, finding applications in diverse domains such as chemical, food, and pharmaceutical industries (Aguilera *et al.*, 1995; Zafar *et al.*, 2017).

The impact of phenomena such as particle swelling or softening on the response of the material can be significant (Glenn *et al.*, 1991; Aguilera *et al.*, 1995; El Youssoufi *et al.*, 2005; Garcia-Rojo *et al.*, 2005; Radjai *et al.*, 2017; Sweijen *et al.*, 2017; Zafar *et al.*, 2017; Aguirre *et al.*, 2021; Braile *et al.*, 2022; Vego, 2023). However, the simultaneous occurrence of these two phenomena is generally overlooked (Sweijen *et al.*, 2017; Braile *et al.*, 2022). The study presented here is inspired by a recent experimental work performed on a highly hydro-sensitive granular material (Vego *et al.*, 2022, 2023a; 2023b), employed as a reference

for assemblies that can exhibit both swelling and softening at the particle scale. Specifically, several samples of couscous were exposed to high relative humidity levels while being subjected to constant vertical stress in oedometric conditions. Information about the evolving microstructure and the water distribution was concurrently gathered by way of X-ray (Vego *et al.*, 2022), neutron + X-ray tomography (Vego *et al.*, 2023b), and time-domain nuclear magnetic resonance (Vego *et al.*, 2023a). In these works, the samples exhibit dilation and compaction, despite the constant vertical stress, as shown in Fig. 1(a). This is ascribed to the concurrent occurrence of swelling and softening at the particle scale. While some single-grain stiffness tests confirm this loss of rigidity of the particles (see Appendix), a link is missing to justify this response. This work aims to fill this gap through numerical simulations investigating the interplay between these concurrent and competing processes.

The modelling approach presented in this paper is intentionally simple, in so much as the response is described through few variables, all described by relatively simple equations. Beginning with elementary assumptions at the particle scale, the final goal is to mimic meso-scale mechanisms observed experimentally and notably the dilation–compaction response (Vego *et al.*, 2022; Vego, 2023; Vego *et al.*, 2023b).

Elementary and computationally efficient two-dimensional (2D) simulations are performed using the discrete element method (DEM). Furthermore, these meso-scale key features emerge even from the simpler model comprising only two particles (1D system).

A SIMPLE DISCRETE APPROACH

Concurrent swelling and softening

Both the swelling and softening phenomena are described as depending from a single governing variable, here denoted as x. This variable – that could be, for example, the water content – is considered *independent* and always positive. In real-case scenarios, x may evolve with time, temperature, or other external factors. This dependency may also be influenced by inherent material properties. For sake of generality, these further possible dependencies are neglected.

A useful and very common simplification is the approximation of the particle shape as spheres, which is also adopted in this study. Taking the particle radius as a metric of the particle size, the swelling dependence on x can be expressed as:

$$r(x) = r_0(1 + \alpha_r x)^{1/3} \text{ for } x \in [0, x_{MAX}] \quad (1)$$

where r indicates the radius of the particle, r_0 is the initial radius (when $x = 0$), and α_r defines the inherent relationship between swelling/shrinking and the governing variable x, for example, water content. This linear relationship between the particle volume and x is supported by experimental results on hygroscopic particles such as couscous (Vego, 2023; Vego *et al.*, 2023a).

To describe then the softening of particles with respect to x, an exponential decay of the particle stiffness k is imposed based on experimental observations, here reported in the Appendix, and on previous studies (Glenn *et al.*, 1991; Kamst *et al.*, 2002; Cao *et al.*, 2004):

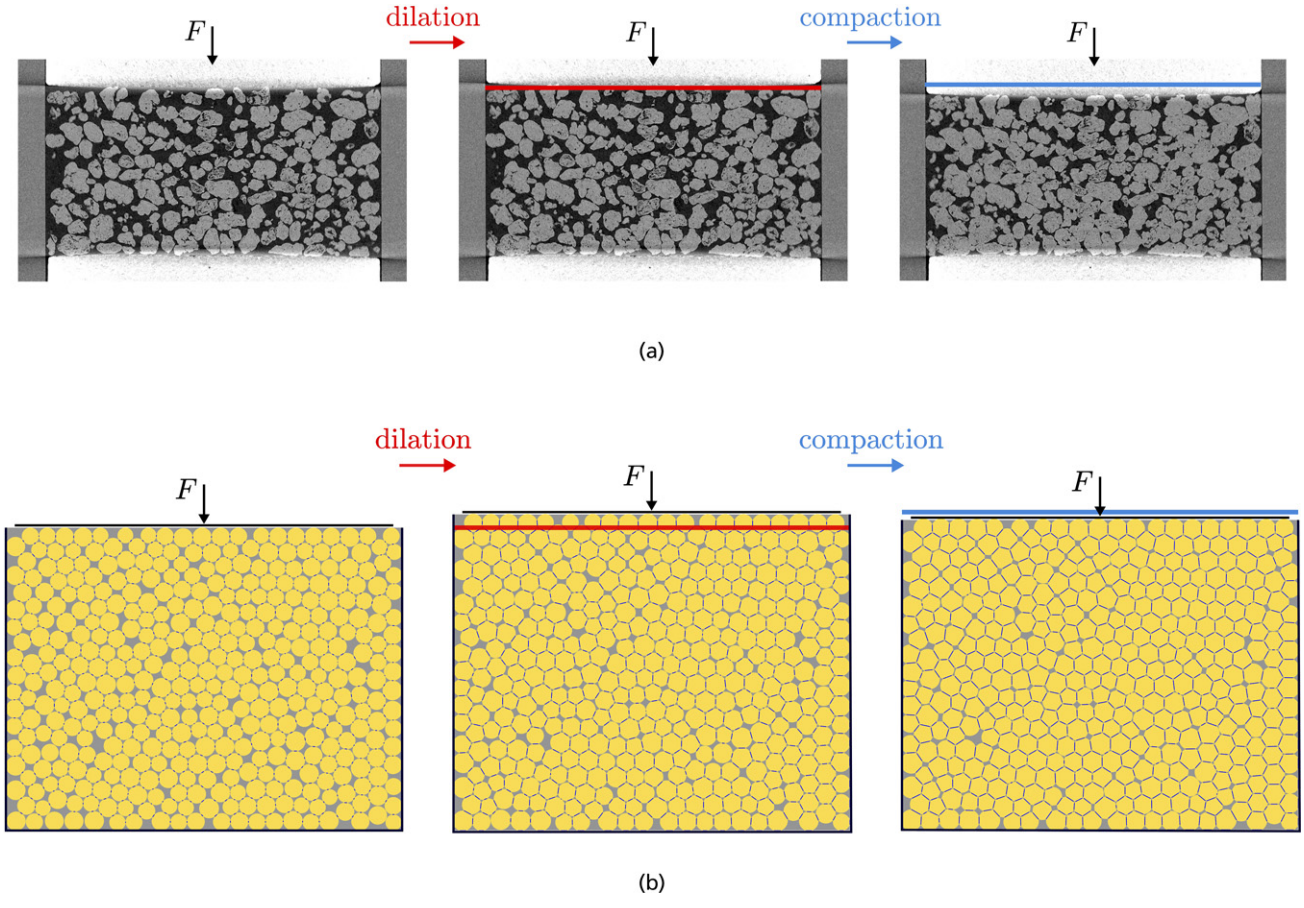

Fig. 1. (a) Tomography images of an assembly of couscous exposed to high relative humidity in a 16 mm diameter oedometer (Vego *et al.*, 2022) and (b) illustration of a 2D DEM simulation. A dilatant–compactant response for assemblies of swelling and softening particles subjected to a constant vertical force $\boldsymbol{F}$ is observed in both the experiment and the simulation. Initially, the swelling induces a dilation of the system. Eventually, when the softening of the particles becomes dominant, the assembly is compacted by the applied vertical force

$$k(x) = k_0\left[\beta_k + (1-\beta_k)e^{-\gamma_k x}\right] \text{ for } x \in [0, x_{MAX}] \quad (2)$$

where k_0 is the stiffness at $x = 0$, and the ratio $\beta_k = k(\infty)/k_0$ indicates the ultimate softening ratio, while the coefficient γ_k modulates the softening rate with x, which is an inherent property of the material of interest. The exponential decrease equation is also chosen for its stability. This way, the stiffness of the particle cannot indefinitely decrease, but rather reach $k(x_{MAX})$ – close to the asymptotic value $k(\infty)$ – when $x \to x_{MAX}$. It could be argued that the stiffness of the particle could increase instead of decreasing; however, this is an unlikely scenario while a volumetric dilation occurs and would contradict most experimental data in the literature.

Two-dimensional DEM simulations

The DEM (Cundall & Strack, 1979) is selected as a numerical technique to assess whether the material model is able to replicate the mechanisms of a particle assembly as observed experimentally. The simulation configuration is as follows.

- A total of 407 spheres of diameter between 625 and 800 μm are restricted in a plane by three rigid walls, under the action of gravity and a constant vertical force applied on the upper wall (see Fig. 1(b)).
- The axial symmetry of oedometric conditions allows for the 2D simplification, where the centres of particles are only allowed to move in a given plane. Despite the 2D restriction for kinematics, the model maintains the 3D nature of the particles for mass/volume and interactions.
- Inter-particle forces are modelled with the Hertz–Mindlin non-linear elastic model, given its widespread adoption and generality, which challenges the assumption of small overlap.
- The contact stiffness is defined as the harmonic mean of that of the two particles.
- The tangential forces are limited through the Coulomb friction criterion.

The next step involves activating the swelling and softening of the particles. This is done imposing a relationship between x and the time-steps of the numerical simulation. The meaning of *time* differs between these numerical DEM simulations and the actual experimental work. Nonetheless, a relatively small time-step is adopted in sequential computations, preserving the quasi-static nature of the problem. The chosen form for the x growth is an exponential increase, a form supported by different studies investigating hygroscopic materials (Omidian *et al.*, 1998; El Youssoufi *et al.*, 2005; De Richter *et al.*, 2022; Vego *et al.*, 2023a, 2023b):

$$x(t) = x_{MAX}(1 - e^{-t/\tau}) \quad (3)$$

where t indicates the time-step, x_{MAX} is the asymptotic x value, and τ is its growth rate; τ is calibrated to reach a value of $x \approx x_{MAX}$ by the end of the simulation.

Before running the simulations, it is necessary to define the particle density ($\rho = 1{\cdot}3$ g/cm^3, in order to match experimental data of couscous) and the friction coefficient ($\mu = 0{\cdot}8$, arbitrarily imposed). The α_k coefficient in Equation 1 is set equal to 1, under the assumption that the density of the particles remains constant, and x represents the water content (Vego, 2023). The stiffness is calibrated as discussed in the Appendix. The parameters selected to perform the sensitivity analysis are summarised in Table 1.

Table 1. Input parameters for the 2D DEM numerical simulations

Simulation parameter	Value
x_{MAX}	0·5
Initial radius r_0	0·31–0·4 mm
Particle density ρ	1·3 g/cm^3
α_r	1
Friction coefficient μ	0·8
Initial particle stiffness k_0	4·29 N/m^2
Softening ratio β_k	0·01
Oedometer width	16 mm

A sensitivity analysis is performed to understand the role of the applied vertical force, using an in-house C++ DEM code. Ten different simulations are run with force values ranging from 0·01 to 5 N. Simulations with exactly $F = 0$ N are not executed because of the lack of stable solutions, although the 0·01 N can be virtually considered as the free-swelling case.

Figure 2 presents the evolution of the relative height of the samples, denoted as $\Delta h/h_0$, where h_0 is the initial height of the assembly and Δh is the difference between the current height at a given simulation step and h_0. Specifically, Fig. 2(a) shows that the response of the assembly with respect to time follows the imposed increase of x in Equation 3 at relatively low loads, while the effects of particle softening become progressively more dominant as the load increases. When studying the evolution of $\Delta h/h_0$ with the independent variable x, one can note again the emergence of a dilation–compaction behaviour and that, for relatively small loads, the response of the assembly can be roughly approximated as linear, given the linear relationship between the particle volume and x (Equation 1), as highlighted by the dashed line in Fig. 2(b).

Despite the simplicity of the model, the simulations – under specific conditions – are capable of reflecting the dilation–compaction behaviour of the assembly observed experimentally (Vego *et al.*, 2022, 2023a, 2023b) as a result of the competition between swelling and softening at the particle scale.

A 1D system to explore the role of variables

Hereafter, a further reduction step is performed to explore the response of swelling and softening of the particles. Starting from the main assumptions made for the 2D model, a simplified 1D analysis is performed.

This new configuration is conceptualised as two identical particles packed vertically in an oedometric cell with diameter equal to $2r_0$. A vertical constant force is applied to the packing: $F = 2r_0p$, where p represents the vertical stress. To counterbalance the applied force F, the single contact force is equilibrated when $K(x)u = 2r_0p$, with u indicating the overlap between the two particles. Therefore, u can be expressed as:

$$u(x) = \frac{2r_0p}{K(x)} \quad (4)$$

The relative variation in height of the system is denoted as ε_n, where n is the direction linking the centres of the two particles. As x increases, so does the particles size, and the expression for ε_n is then given by:

$$\varepsilon_n(x) = \frac{[r(x) - u(x)] - (r_0 - u_0)}{r_0 - u_0} \quad (5)$$

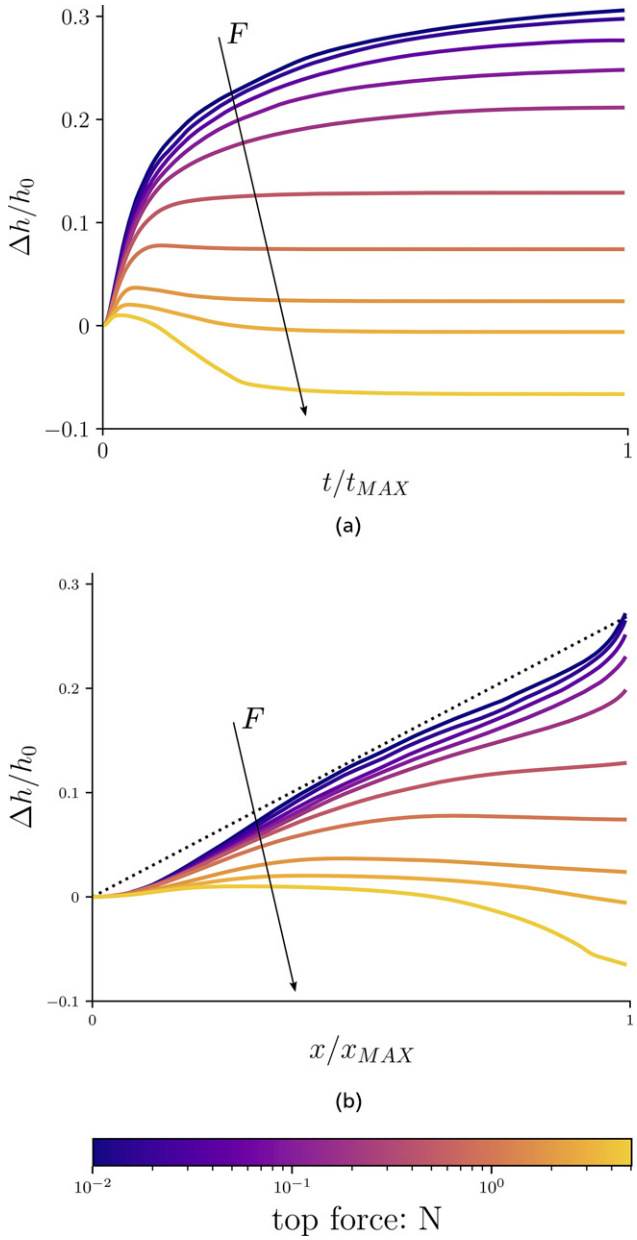

Fig. 2. Vertical load sensitivity analysis: (a) evolution of the sample relative height variation ($\Delta h/h_0$) as a function of the time-step and (b) the main variable x. Given the generality of the model, both the time-step and the x values have been normalised. For relatively small vertical loads, the assembly dilates coherently with the swelling of particles. The softening effect becomes significant when for higher values of F, the vertical force applied on the upper wall: the concurrent swelling and softening at the particle scale induces a dilatant–compactant response of the assembly

where the derivation of this expression can be deduced from the sketch in Fig. 3. It should be noted that a positive value of ε_n indicates a dilation of the system and vice versa. Moreover, the picture does not take into consideration any micro-structural features, as the emphasis lies solely on the inter-particle contact in one and only one direction.

Substituting the terms from Equations 1 and 2 – assuming that the stiffness of the 1D system decreases similarly to the one of individual particles – two distinct components are identified in the expression for ε_n:

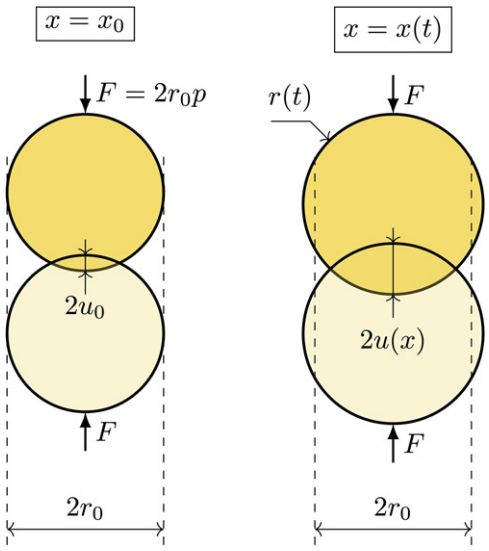

Fig. 3. Illustration depicting the parameters employed in the two-particles system. The direction n is vertical. The centre-to-centre distance is $2[r(x) - u(x)]$

$$\varepsilon_n(x) = \underbrace{\frac{K_0}{K_0 - 2p}\left[(1+\alpha_r x)^{\frac{1}{3}} - 1\right]}_{\varepsilon_{\text{swelling}}} - \underbrace{\frac{2p}{K_0 - 2p}\left[\frac{(1-\beta_K)(1-e^{-\gamma_K x})}{\beta_K + (1-\beta_K)e^{-\gamma_K x}}\right]}_{\varepsilon_{\text{softening}}} \tag{6}$$

The first term reflects the contribution from the swelling of the particles, while the second term their softening. Notably, the initial radius r_0 does not appear in the final equation, indicating the independence from particle size.

Equation 6 allows for quantifying the role played by these competing mechanisms. To understand the load discerning between a dilatant and a compactant response, one can compute the first derivative of the height variation ε_n with respect to the main variable x:

$$\begin{aligned}\frac{\mathrm{d}\varepsilon_n}{\mathrm{d}x}(x) = &\underbrace{\frac{K_0}{K_0 - 2p}\,\frac{\alpha_r}{3(1+\alpha_r x)^{2/3}}}_{\frac{\mathrm{d}}{\mathrm{d}x}\varepsilon_{\text{swelling}}} \\ &\underbrace{-\frac{2p\gamma_K(1-\beta_K)}{K_0 - 2p}\,\frac{e^{-\gamma_K x}}{[\beta_K + (1-\beta_K)e^{-\gamma_K x}]^2}}_{\frac{\mathrm{d}}{\mathrm{d}x}\varepsilon_{\text{softening}}}\end{aligned} \tag{7}$$

At $x = 0$, one obtains:

$$\begin{aligned}\frac{\mathrm{d}\varepsilon_n}{\mathrm{d}x}(0) &= \underbrace{\frac{K_0\alpha_r}{3(K_0 - 2p)}}_{\frac{\mathrm{d}}{\mathrm{d}x}\varepsilon_{\text{swelling}}(0)} - \underbrace{\frac{2p\gamma_K(1-\beta_K)}{K_0 - 2p}}_{\frac{\mathrm{d}}{\mathrm{d}x}\varepsilon_{\text{softening}}(0)} \\ &= \frac{\alpha_r K_0 + 6\gamma_K(\beta_K - 1)p}{3(K_0 - 2p)}\end{aligned} \tag{8}$$

The sign of $\frac{\mathrm{d}\varepsilon_n}{\mathrm{d}x}(x)$ is determined by the right-hand side of the expression above. Furthermore, if the condition $K_0 \gg 2p$ holds – a likely condition in most real-case scenarios – the stress value at which the system neither grows nor decreases in size, that is, $\frac{\mathrm{d}\varepsilon_n}{\mathrm{d}x}(x) = 0$, can be defined as the reference vertical stress $\hat{p}$:

$$\hat{p} = \frac{\alpha_r K_0}{6(1-\beta_K)\gamma_K} \tag{9}$$

This provides an indication of the vertical stress above which initial dilation of the system does not occur and vice versa.

CONCLUSIONS AND PERSPECTIVES

This contribution studies the macroscopic response and microscopic origins of the concurrent swelling and softening of particles, a common process in natural and artificial materials, which is often overlooked in the literature. A simple model that takes into account the simultaneous occurrence of these phenomena is developed based on micro- and macro-scale experimental observations. This model is intentionally simple and all variables depend on a main parameter, x. Numerical simulations using the DEM are performed to verify whether the model is able to capture key features observed experimentally. The approach can be considered successful, as it can capture the dilatant–compactant response. The sensitivity study reveals a range of loads for which this can occur in 2D oedometric conditions. An analytical 1D model based on two particles is then developed to further explore the role that certain variables play in the response of assemblies of swelling and softening particles. This further simplification of the problem captures complex processes observed in experiments and provides, in a first approximation, an insight into the parameters governing the response.

To summarise, the simplicity of the modelling approach adopted in this study is an intentional choice made to demonstrate that certain mesoscopic scale mechanisms emerge from the basic processes occurring at the particle scale. The model can serve as an intuitive and effective pedagogical tool, showing that complex responses can be initiated by elementary particle-to-particle interactions.

Several key improvements of the model, directly associated with swelling and softening particles, could include: (*a*) an appropriate inter-particle contact law, which also accounts for cohesion, as it plays an important role in granular assemblies (Delenne *et al.*, 2009; Sonzogni *et al.*, 2024), (*b*) explicitly incorporating particle deformability, possibly based on the recent advances in the modelling of the interaction among deformable particles (Cárdenas-Barrantes *et al.*, 2021, 2022), rather than allowing a large interpenetration, (*c*) taking into account inevitable heterogeneity in the activation of swelling and softening (Brockbank *et al.*, 2021; Vego *et al.*, 2022; Vego, 2023; Vego *et al.*, 2023a), and (*d*) analysing different forms of input functions for radius and stiffness.

CONFLICTS OF INTEREST

There are no conflicts to declare.

ACKNOWLEDGEMENTS

This project has received funding from the European Union's Horizon 2020 research and innovation program under the Marie Skłodowska-Curie Grant agreement No. 812638 (CALIPER). The authors acknowledge LabEx Tec 21-France (Investissements d'Avenir #ANR-11-LABX-0030).

Appendix

Stiffness of Individual Couscous Particles VS. Water Content

Building upon the previously mentioned work (Vego *et al.*, 2022, 2023a, 2023b), an experimental campaign is conducted to evaluate the dependency of the stiffness of individual couscous particles to their water content (w). Specifically, compression tests of individual couscous particles are performed at different levels of water content. This appendix summarises the experimental procedure in the next section, while the last section presents relevant results for the sensitivity study presented in the main text, particularly for the calibration of the particle stiffness k and its softening rate γ_k.

Experimental procedure

Couscous particles, whose diameter is between 625 and 800 μm, are placed in a sealed vessel and exposed to a continuous flow of air of constant relative humidity to stabilise their water content (Vego *et al.*, 2023a). This process is repeated for increasing humidity levels until a constant w is recorded. Then, only relatively convex particles are selected and placed in a custom-built apparatus, where they are compressed by moving a piston at constant and slow velocity ($v = 1$ μm/s). This piston, whose displacement is controlled by an ultra-high precision linear actuator with ceramic linear motor, is securely connected to a load cell.

The experimental campaign includes simple and cyclic compression tests. The simple tests are performed as described above, while the cyclic ones require additional steps in the compression stage. In this latter case, the piston is halted once the load cell records a force increase. The system is then left to relax for 3 min, after which the particle is 'unloaded' back to the position corresponding to the first halt (displacement of 0 μm). Next, the particle is compressed again by imposing a displacement equal to +10 μm relative to the maximum displacement of the previous cycle. In total, seven cycles are performed.

Results

The simple compression tests are performed at five different water contents: 4·05, 7·89, 9·80, 11·55, and 18·1%. For each w, at least nine successful tests are conducted in order to average them.

Figure 4 reports, for each w, the evolution of force–displacement curves within a 25 μm displacement range, ≈3·5% of the average particle diameter. Drier particles exhibit higher stiffness. In addition, the variance is larger for low w due to more brittle response. The collected data suggest that the force and displacement are linearly related within the selected range.

The force–displacement curves then allow for measuring the apparent stiffness $\widetilde{k}$ of the particles, defined as the ratio between the average force and the respective displacement.

It should be noted that the apparent stiffness determined from these compression tests cannot be directly used as a value for k in the sensitivity study. Therefore, an indication of the stiffness value and its evolution is obtained by deliberately dividing the apparent stiffness by the average particle diameter $2\bar{r}$ (Zhang *et al.*, 2016). As highlighted in Fig. 5, $\widetilde{k}$ decreases with w, a behaviour similar to that observed in previous experimental studies exploring the mechanics of other hygroscopic materials (Glenn *et al.*, 1991; Kamst *et al.*, 2002; Cao *et al.*, 2004). A negligible difference is observed among different displacement ranges.

The cyclic tests are carried out to qualitatively investigate the loading–unloading response and the variation of the stiffness of particles undergoing cyclic loading. Here, the results of two cyclic compression tests are reported; the first test is performed on a relatively dry particle with $w = 4\%$, while the second test on a more hydrated one ($w = 10\%$). The force–displacement curves of these two tests are reported in Figs. 6(a) and 6(b), respectively. The results suggest that $\widetilde{k}$ does not vary between

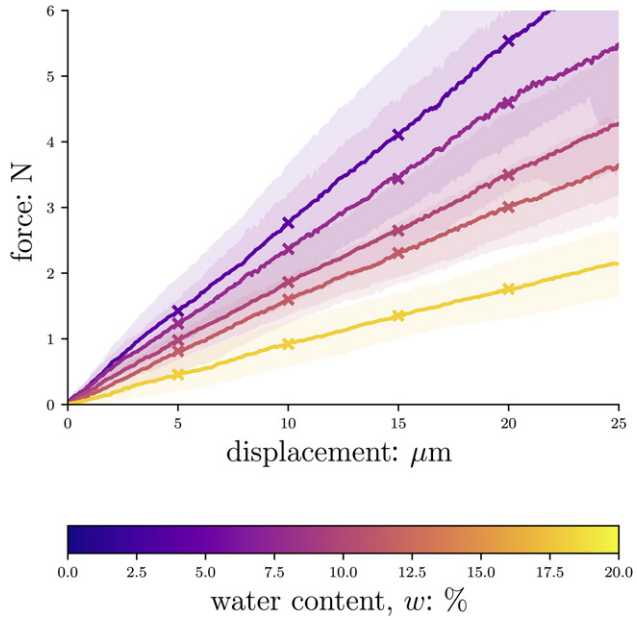

Fig. 4. Force–displacement curves from the simple compression tests of individual couscous particles at different water content levels (from 4·05% to 18·1%). Drier particles exhibit a higher stiffness than wet ones. The force–displacement response can be described as a linear relation

cycles up to the fifth cycle, after which the particle is most likely severely damaged. Further dependencies of the harmonic stiffness adopted in the Hertz–Mindlin model can be then neglected in first approximation. Moreover, the drier particle shows a fragile breakage, while the other exhibits a more ductile response.

Notably, these cyclic compression tests show loss of linearity upon cycling loading and unloading, which is not crucial to capture the key macroscopic process of interest here (dilation and compaction of the sample upon constant load), but which could constitute an interesting future generalisation of the model.

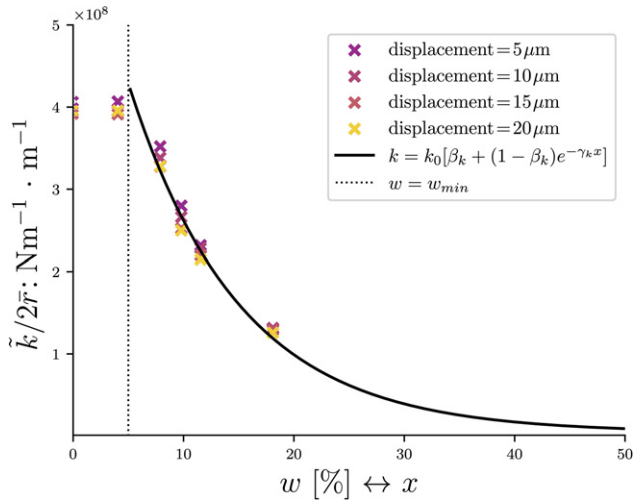

Fig. 5. Couscous particles stiffness $\tilde{k}/2\,\bar{r}$ (apparent stiffness/average diameter) as a function of water content w. The particles soften at higher water content levels. The effect of the piston displacement range is found to be negligible. A plausible fit with Equation 2 is shown as a dotted black line

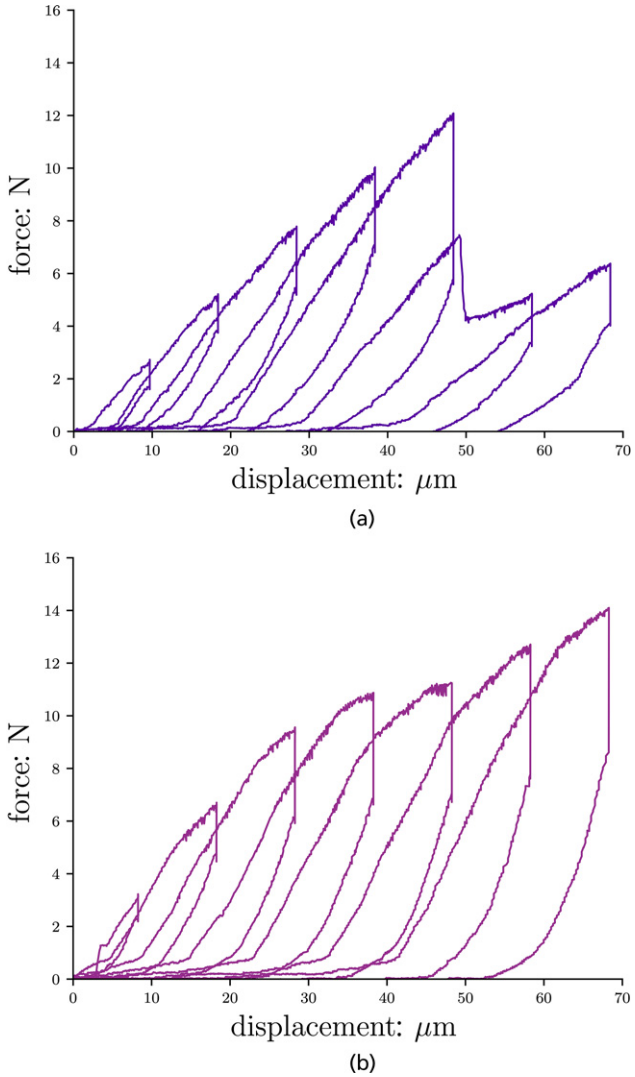

Fig. 6. Force–displacement curves of cyclic compression tests at different water content levels: (a) $w = 4\%$ and (b) $w = 10\%$. The loading and unloading apparent stiffness appear to remain constant throughout the tests

REFERENCES

Aguilera, J. M., del Valle, J. M. & Karel, M. (1995). Caking phenomena in amorphous food powders. *Trends in Food Science & Technology* **6**, No. 5, 149–155, https://doi.org/10.1016/S0924-2244(00)89023-8.

Aguirre, M. A., Luding, S., Pugnaloni, L. A. & Soto, R. (2021). Powders & grains 2021. 9th International Conference on Micromechanics of Granular Media. *EPJ Web Conf* **249**, 00001, https://doi.org/10.1051/epjconf/202124900001.

Braile, D., Hare, C. & Wu, C.-Y. (2022). DEM analysis of swelling behaviour in granular media. *Adv Powder Technol* **33**, No. 11, 103806, https://doi.org/10.1016/j.apt.2022.103806.

Brockbank, K., Armstrong, B. & Clayton, J. (2021). Measurement and quantification of caking in excipients and food products with emphasis on the non-homogeneous interaction with ambient moisture. *Particuology* **56**, 75–83, https://doi.org/10.1016/j.partic.2020.10.012.

Cao, W., Nishiyama, Y. & Koide, S. (2004). Physicochemical, mechanical and thermal properties of brown rice grain with various moisture contents. *Int J Food Sci Tech* **39**, No. 9, 899–906, https://doi.org/10.1111/j.1365-2621.2004.00849.x.

Cárdenas-Barrantes, M., Cantor, D., Barès, J., Renouf, M. & Azéma, E. (2021). Micromechanical description of the compaction of soft pentagon assemblies. *Phys Rev E* **103**, No. 6–1, 062902, https://doi.org/10.1103/PhysRevE.103.062902.

Cárdenas-Barrantes, M., Cantor, D., Barès, J., Renouf, M. & Azéma, E. (2022). Three-dimensional compaction of soft

granular packings. *Soft Matter* **18**, No. 2, 312–321, https://doi.org/10.1039/D1SM01241J.

Cundall, P. A. & Strack, O. D. L. (1979). A discrete numerical model for granular assemblies. *Géotechnique* **29**, No. 1, 47–65, https://doi.org/10.1680/geot.1979.29.1.47.

De Richter, S. K., Gaudel, N., Gaiani, C., Pascot, A., Ferrari, M. & Jenny, M. (2022). Swelling of couscous grains under saturated conditions. *J Food Eng* **319**, 110910, https://doi.org/10.1016/j.jfoodeng.2021.110910.

Delenne, J.-Y., Topin, V. & Radjai, F. (2009). Failure of cemented granular materials under simple compression: experiments and numerical simulations. *Acta Mech* **205**, No. 1–4, 9–21, https://doi.org/10.1007/s00707-009-0160-9.

El Youssoufi, M. S., Delenne, J.-Y. & Radjai, F. (2005). Self-stresses and crack formation by particle swelling in cohesive granular media. *Phys Rev E Stat Nonlin Soft Matter Phys* **71**, No. 5 Pt 1, 051307, https://doi.org/10.1103/PhysRevE.71.051307.

Garcia-Rojo, R., Herrmann, H. J. & McNamara, S. (2005). Powders & grains. In *Proceedings of the 5th International Conference on Micromechanics of Granular Media*, https://doi.org/10.1201/NOE0415383486.

Glenn, G. M., Younce, F. L. & Pitts, M. J. (1991). Fundamental physical properties characterizing the hardness of wheat endosperm. *J Cereal Sci* **13**, No. 2, 179–194, https://doi.org/10.1016/S0733-5210(09)80035-0.

Kamst, G. F., Bonazzi, C., Vasseur, J. & Bimbenet, J. J. (2002). Effect of deformation rate and moisture content on the mechanical properties of rice grains. *Trans ASAE* **45**, No. 1, 145, https://doi.org/10.13031/2013.7857.

Kolb, E., Quiros, M., Meijer, G. J., Bogeat-Triboulot, M. B., Carminati, A., Andò, E., Sibille, L. & Anselmucci, F. (2022). Root–soil interaction. In *Soft Matter in Plants: From Biophysics to Biomimetics* (eds K. Jensen and Y. Forterre), pp. 165–202. Royal Society of Chemistry, https://doi.org/10.1039/9781839161162-00165.

Omidian, H., Hashemi, S. A., Sammes, P. G. & Meldrum, I. (1998). A model for the swelling of superabsorbent polymers. *Polymer* **39**, No. 26, 6697–6704, https://doi.org/10.1016/S0032-3861(98)00095-0.

Radjai, F., Nezamabadi, S., Luding, S. & Delenne, J.-Y. (2017). Powders and grains 2017. *EPJ Web of Conferences 140*. See https://www.epj-conferences.org/articles/epjconf/abs/2017/09/contents/contents.html.

Romero, E., Della Vecchia, G. & Jommi, C. (2011). An insight into the water retention properties of compacted clayey soils. *Géotechnique* **61**, No. 4, 313–328, https://doi.org/10.1680/geot.2011.61.4.313.

Saha, A., Sekharan, S. & Manna, U. (2020). Superabsorbent hydrogel (SAH) as a soil amendment for drought management: a review. *Soil and Tillage Research* **204**, 104736, https://doi.org/10.1016/j.still.2020.104736.

Sonzogni, M., Vanson, J.-M., Ioannidou, K., Reynier, Y., Martinet, S. & Radjai, F. (2024). Dynamic compaction of cohesive granular materials: scaling behavior and bonding structures. *Soft Matter* **20**, No. 27, 5296–5313, https://doi.org/10.1039/D3SM01116J.

Sweijen, T., Chareyre, B., Hassanizadeh, S. M. & Karadimitriou, N. K. (2017). Grain-scale modelling of swelling granular materials; application to super absorbent polymers. *Powder Technol* **318**, 411–422, https://doi.org/10.1016/j.powtec.2017.06.015.

Vego, I. (2023). Multi-modal investigation of hygroscopic granular media at high relative humidity. PhD thesis, Université Grenoble Alpes. https://theses.hal.science/tel-04360890.

Vego, I., Tengattini, A., Andò, E., Lenoir, N. & Viggiani, G. (2022). The effect of high relative humidity on a network of water-sensitive particles (couscous) as revealed by in situ X-ray tomography. *Soft Matter* **18**, No. 25, 4747–4755, https://doi.org/10.1039/D2SM00322H.

Vego, I., Benders, R. T., Tengattini, A., Vergeldt, F. J., Dijksman, J. A. & van Duynhoven, J. P. M. (2023a). Heterogeneous swelling of couscous particles exposed to a high relative humidity air, as revealed by TD-NMR and X-ray tomography. *Food Structure* **37**, 100330, https://doi.org/10.1016/j.foostr.2023.100330.

Vego, I., Tengattini, A., Lenoir, N. & Viggiani, G. (2023b). The influence of water sorption on the microstructure of a hydro-sensitive granular material (couscous) deduced from simultaneous neutron and X-ray tomography. *Granular Matter* **25**, No. 4, 65, https://doi.org/10.1007/s10035-023-01356-5.

Zafar, U., Vivacqua, V., Calvert, G., Ghadiri, M. & Cleaver, J. A. S. (2017). A review of bulk powder caking. *Powder Technology* **313**, 389–401, https://doi.org/10.1016/j.powtec.2017.02.024.

Zhang, Y. D., Buscarnera, G. & Einav, I. (2016). Grain size dependence of yielding in granular soils interpreted using fracture mechanics, breakage mechanics and Weibull statistics. *Géotechnique* **66**, No. 2, 149–160, https://doi.org/10.1680/jgeot.15.P.119.